

A Polarizable Model for Ethylene Oxide

Raymond D. Mountain

J. Phys. Chem. B, **2005**, 109 (27), 13352-13355 • DOI: 10.1021/jp051379k • Publication Date (Web): 18 June 2005

Downloaded from <http://pubs.acs.org> on March 4, 2009

More About This Article

Additional resources and features associated with this article are available within the HTML version:

- Supporting Information
- Access to high resolution figures
- Links to articles and content related to this article
- Copyright permission to reproduce figures and/or text from this article

[View the Full Text HTML](#)



ACS Publications
High quality. High impact.

A Polarizable Model for Ethylene Oxide

Raymond D. Mountain*

Physical and Chemical Properties Division, Chemical Science and Technology Laboratory,
National Institute of Standards and Technology, Gaithersburg, Maryland 20899-8380

Received: March 16, 2005; In Final Form: May 18, 2005

A series of interaction models for ethylene oxide are developed for use in molecular simulation of the thermal properties of both the gas and liquid phases. While it is possible to develop nonpolarizable models to accurately generate either the gas or liquid properties separately, it was not possible to do so using a single model for both phases. A polarizable, rigid all-atom model was developed that reproduces the temperature dependence of the second virial coefficient $B(T)$ and the pressure of the liquid at ambient conditions. The model consists of Lennard-Jones and Coulomb interactions between intermolecular atomic sites plus a scalar polarizability located at the midpoint of the line joining the carbon sites. The electrostatic charges and the polarizability are set to match the experimentally determined dipole and quadrupole moments and the molecular polarizability.

1. Introduction

Molecular simulation methods, such as molecular dynamics and Monte Carlo, hold great promise for providing the means to predict thermophysical properties of fluids in regions where experimental data are not available. These methods require an accurate representation of molecular interactions if they are to generate thermophysical properties that are physically accurate. The methods for developing interaction models in terms of potential functions and polarization terms are not uniquely determined and involve varying degrees of empiricism. Ab initio quantum methods are capable of determining intramolecular properties with good accuracy, but are less capable of determining intermolecular interactions.

In this note, we discuss the development of a model for the intermolecular interaction of the three-member ring molecule ethylene oxide [(CH₂)₂O]. Ethylene oxide is an important industrial chemical used in the production of a variety of other compounds.^{1,2} It is flammable and toxic so considerable care must be exercised in its use. These features make it a candidate for using simulations as an alternative to laboratory exploratory studies. The model developed here is able to reproduce both gas phase and liquid-phase properties of ethylene oxide. The model building process uses ab initio and experimental results for the electrostatic part of the intermolecular interactions, for the molecular polarizability, and for the geometry of the molecule. The multipole moments, the polarizability, and the geometry obtained from high level quantum chemistry calculations are in good agreement with the experimentally derived quantities.³ The semiempirical component of the method involves the use of measured fluid properties. The fluid properties used in the development of the model are the temperature dependence of the second virial coefficient, $B(T)$,^{4,5} and the pressure (≈ 0.1 MPa.) of the liquid for the density 0.9 g/cm³ at 273 K.⁶ The objective is for the calculated values of $B(T)$ to coincide with the experimentally derived ones over the temperature interval 250 to 600 K within 5% (the estimated uncertainty in $B(T)$ ⁵) and for the calculated liquid pressure to be within 2 MPa of the measured value. In addition to the fluid

properties, the placement of the charges and the polarizability are other aspects of the model that are not based on ab initio methods. The purpose for developing this model is to permit the use of molecular simulation methods to estimate properties of the fluid at elevated temperatures and pressures.

In the following sections, three models of increasing complexity are examined. These are a united-atom model taken from the literature,⁷ an all-atom model and an all-atom model with fixed charges and explicit polarizability. Only the last model is able to satisfy the specified conditions for $B(T)$ and the liquid pressure.

2. A United-Atom Model

There is one simulation of liquid ethylene oxide reported in the literature.⁷ We briefly discuss the predictions of this model. It employed a united-atom, 3-site model and was concerned primarily with the dielectric properties of the liquid. The interactions were of the site–site Lennard-Jones potentials plus site–site Coulomb form. The charges on the united atom sites were selected to reproduce the dipole moment of a molecule (1.89 D)⁸ with the experimentally determined geometry for the carbon and oxygen sites. Two parametrizations of the Lennard-Jones potential, version A and version B, were considered. Version A produced the liquid pressure that was in serious error, while version B provided a sensible but not particularly accurate value for the pressure for the liquid density^{6,9} at 260 K. We determined the second virial coefficient for both versions of the model by evaluating

$$B(T) = -\frac{1}{2} \int \langle \exp(-\beta u(\mathbf{r}, \omega_1, \omega_2)) - 1 \rangle_{\omega_1, \omega_2} d\mathbf{r} \quad (1)$$

where $u(\mathbf{r}, \omega_1, \omega_2)$ is the potential energy of a pair of molecules and the angular brackets indicate an average over the orientation ω_1, ω_2 of the two molecules separated by \mathbf{r} .¹⁰ The integral is evaluated using a Monte Carlo integration scheme written specifically for this task. Both parametrizations fail to accurately predict the temperature variation of the second virial coefficient as indicated in Figure 1.

* Corresponding author Email; RMountain@nist.gov.

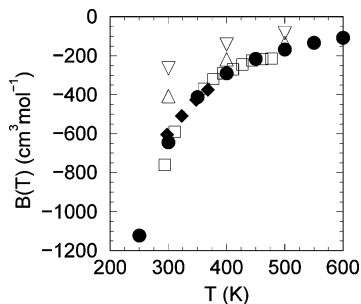


Figure 1. Second virial coefficient for ethylene oxide as determined by various groups: solid circles,⁵ solid diamonds,⁴ open squares.¹¹ The open triangle pointing up results from the model of Version A and open triangle pointing down result from the model of Version B described in ref 7.

3. An All-Atom Model

The simulations described in this and the following section were performed on a system of 216 molecules. The edge of the cubic simulation cell was fixed at 2.6 nm so that the desired density of 0.9 g/cm³ was realized. The temperature of the system was maintained at 273 K by thermostats for the translational and orientational degrees of freedom.¹² The equations of motion were integrated using a Velocity Verlet algorithm¹³ with a time step of 1 fs. The simulations were run for at least 200 ps so that reliable estimates for the pressure were obtained.

Since a united-atom model proved to be inadequate to represent both the vapor and liquid phases, we next examine an all-atom model with the hydrogen sites located at the positions determined by quantum chemistry computations.³ The initial interaction model used the same functional form as the united-atom model, namely Lennard-Jones plus Coulomb interactions between sites on distinct molecules

$$\phi_{ij}(r) = 4\epsilon_{ij}[(\sigma_{ij}/r)^{12} - (\sigma_{ij}/r)^6] + q_i q_j / r \quad (2)$$

where i and j indicate sites on different molecules (O, C, H) and r is the distance between the sites. The long-range part of the Coulomb interaction is determined using the Ewald summation method.¹⁴ The Lennard-Jones interactions were truncated at 1.3 nm.

The individual molecules are taken to be rigid bodies. The values of the point charges on the sites were selected so that the dipole moment⁸ and the symmetry axis component of the quadrupole moment¹⁵ were consistent with the experimental values. The charges are not varied when determining the other potential parameters. Since the molecule is electrically neutral and there are three types of sites (oxygen, carbon, hydrogen), these conditions determine a unique set of charges. The atom site coordinates in a body fixed coordinate system that are consistent with the geometry of the isolated molecule³ and that diagonalizes the inertial tensor of the molecule and the charges on the sites are listed in Table 1.

Next, Lennard-Jones parameters, ϵ_{ij} and σ_{ij} were developed so that either the pressure at 273 K and density of 0.9 g/cm³ was small or so that the temperature dependence of the second virial coefficient was consistent with the measured coefficients. It was not possible to find a set of parameters that simultaneously did both. The starting point in the process of determining the ϵ_{ij} and σ_{ij} was based on the parameter values of Version A mentioned in section 2.

It might be possible to improve the overall agreement with the experimental results by allowing the charges to be adjustable parameters. This mean field approach to induction effects was

TABLE 1: Body-Fixed Site Coordinates with the Center of Mass at the Origin and Charges for the Ethylene Oxide Molecule

site	x, nm	y, nm	z, nm	q_i (e)
O	0.0799	0.0000	0.0000	-0.1842
C	-0.0426	0.0733	0.0000	-0.3079
C	-0.0426	-0.0733	0.0000	-0.3079
H	-0.0636	0.1310	0.0910	0.2000
H	-0.0636	0.1310	-0.0910	0.2000
H	-0.0636	-0.1310	-0.0910	0.2000
H	-0.0636	-0.1310	0.0910	0.2000

not considered, as it would break the connection with the experimental values for the dipole and quadrupole moments.

4. A Polarizable, All-Atom Model

The next step in the model development is to introduce explicit polarizability into the model, keeping the fixed charges listed in Table 1 unchanged. The scalar polarizability, α , of ethylene oxide is, from quantum chemistry calculations,³ in the range $25a_0^3$ to $30a_0^3$ where a_0 is the Bohr radius, 0.0529 nm. This is in good agreement with the experimental value of the polarizability of 4.9×10^{-40} C² m² J⁻¹.¹⁶ In what follows, $30a_0^3$ was used as the value of the polarizability. The polarizability is placed on the midpoint of the line joining the carbon sites. Other positions were examined, but this position provided the best agreement of the calculated pressure of the liquid and the temperature dependence of the second virial coefficient experiment.

Induced polarization introduces an additional term in the energy of the system of the form

$$E_{\text{pol}} = -\frac{1}{2} \sum_{i=1,N} \vec{\mu}_i \cdot \vec{E}_i^0 \quad (3)$$

where \vec{E}_i^0 is the electric field at site i due to charges on the other molecules and $\vec{\mu}_i$ is the induced moment at site i when the induced moments are obtained as self-consistent solutions of

$$\vec{\mu}_i = \alpha \vec{E}_i^0 + \alpha \sum_{j \neq i} \mathcal{T}_{ij} \vec{\mu}_j \quad (4)$$

where \mathcal{T}_{ij} is the dipole tensor.¹⁷ Since $\vec{\mu}_i$ depends on the induced moments of all of the molecules, induction is a many-body effect. Accurate, stable solutions for the induced moments are realized with six iterations of the coupled equations.¹⁸ This increases the simulation time by a factor of 2 or 3 compared with the case where no induction is present. The ‘‘polarizability catastrophe’’ that occurs when polarization sites get too close together¹⁹ is prevented by the strongly repulsive forces present at small separations.

With induced moments and the parameters in listed in Table 2, it is possible to obtain accurate values for the second virial coefficient over the temperature interval 250 to 600 K and the pressure of the liquid within 2 MPa of zero. The initial ϵ values and σ values were based on the parameters developed in section 3. These parameters were then modified to improve the agreement between the calculated and measured values of $B(T)$. A check on the desirability of the changes was made by determining the pressure of the liquid. This process was continued until the parameters in Table 2 were obtained.

The results for the pressure of the liquid are shown in Figure 2. The cumulative time average value of the pressure (solid line) and 1 ps duration block averages of the pressure (solid circles)

TABLE 2: Lennard-Jones Parameters that Provide the Correct Temperature Dependence of the Second Virial Coefficient and the Liquid Pressure for the Polarizable Model

sites ^a	ϵ/k_B , K	σ , nm
O–O	78.24	0.3002
C–C	70.42	0.2686
H–H	56.72	0.2405
O–C	58.68	0.2923
O–H	53.20	0.2733
C–H	49.90	0.2496

^a O, C, and H stand for the oxygen, carbon, and hydrogen sites, respectively.

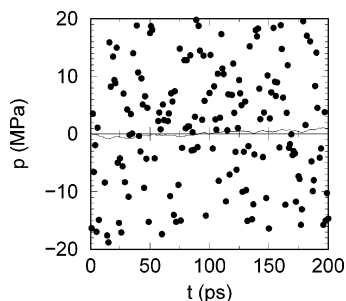


Figure 2. Computed pressure of the liquid shown as a function of time. The solid line is the time averaged cumulative pressure and the solid circles are 1 ps duration block averages.

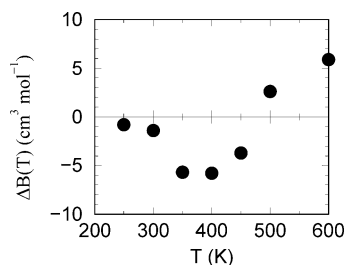


Figure 3. Difference of the computed values of the second virial coefficient from the measured values over the temperature interval 250 to 600 K.

show that the fluctuations in the calculated pressure are large. The long time average is 0.82 MPa. The root-mean-square average value of the induced moment in a molecule is 1.76×10^{-30} C m (0.524 D), about one-fourth the magnitude of the permanent dipole moment (1.89 D). The two vectors are not collinear. The distribution of the angles between the two vectors is strongly peaked at small angles, although the distribution is broad and covers the entire interval between 0° and 180° . The average angle is 40° .

The deviations of the computed second virial coefficient from the values derived from ultrasonic measurements⁵ are shown in Figure 3. The experimentally determined and calculated values agree within 5%. The largest deviation occurs at 400 K. The variability of the calculated values of $B(T)$ for 10 different seed values for the random number generator used in the Monte Carlo program is at most $3 \text{ cm}^3 \text{ mol}^{-1}$.

The sensitivity of the calculated values of the liquid-state pressure and of the second virial coefficient to the Lennard-Jones parameters is estimated by increasing σ_{HH} , σ_{OH} , or σ_{CH} by one percent and repeating the simulation. For the liquid pressure, increasing σ_{HH} by one percent increases the pressure by 18 MPa, increasing σ_{OH} by one percent increases the pressure by 38 MPa, while increasing σ_{CH} by one percent results in no change in the pressure. The corresponding changes in the second virial coefficient are shown in Figure 4. Clearly, these properties

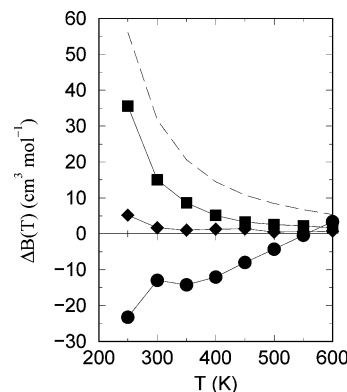


Figure 4. Changes in $B(T)$ resulting from a one percent increase in one of the Lennard-Jones σ values. The circles are for σ_{CH} , the squares are for σ_{OH} , and the diamonds are for σ_{HH} . The dashed line indicates a magnitude of 5% of the calculated value of $B(T)$ using the parameters in Table 2.

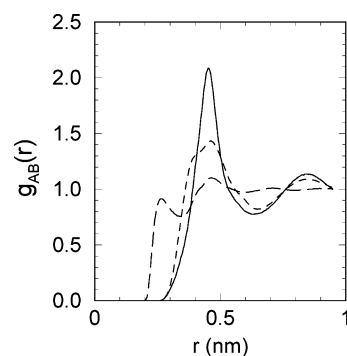


Figure 5. Site–site pair functions for the O–O (solid line), C–C (short dashed line) and H–H (long dashed line) cases for the liquid.

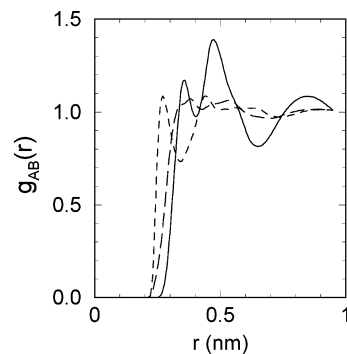


Figure 6. Site–site pair functions for the O–C (solid line), O–H (short dashed line), and C–H (long dashed line) cases for the liquid.

are quite sensitive to the σ values. A similar test with the ϵ values being varied showed that the properties are less sensitive to those quantities.

The choice of which parameters to vary is guided by the liquid-state site–site pair functions that are shown in Figures 5 and 6. The HH, OH, and CH functions indicate that these pairs of sites have the closest encounters and therefore are going to more strongly influence the calculated pressure. That the OH and CH pairs do so is also readily understood in terms of the Coulomb interaction of unlike sign charges. The HH pairs are necessarily close if the CH pairs are close, despite the Coulomb repulsion between H-sites. While these remarks provide a basis for understanding which parameters are going to influence the pressure most strongly, there is a balance between several terms and a direct check on sensitivity is required.

5. Discussion

The sequence of steps followed in developing the polarizable model are predicated on the assumption that it is important to have a physically sound representation of the electrostatic interactions. To this end, the experimentally and computationally determined coordinates of the atom sites were selected. Then charges were placed on the atom sites such that the experimentally determined dipole and quadrupole moments of the molecule were reproduced. The use of discrete charges is an approximation to the actual charge distribution in the molecule. In this case, it appears to provide a satisfactory representation. Quantum chemistry calculations generate a charge distribution. Various schemes for assigning discrete charges from the full distribution do not lead to unique sets of charges, so using the moments to determine the charges has less ambiguity in the values of the charges, although the placement of the charges is still an arbitrary feature.

When it was found that no set of Lennard-Jones parameters was able to provide both the temperature dependence of the second virial coefficient and the liquid pressure for the all-atom model discussed in section 3, the next step in developing the model was to introduce a scalar polarizability at the midpoint of the line joining the carbon sites. The value of the polarizability is consistent with both experimentally based estimates and with quantum chemical calculations. This is the simplest way to deal with the charge rearrangement due to the presence of other molecules. More complex schemes are possible, such as placing multiple polarization sites on bonds. Again, any of these schemes have arbitrary features so going with the simplest one has merit.

The dielectric constant ϵ of the polarizable model was determined using the fluctuation expression¹⁴

$$\epsilon = 1 + \frac{4\pi\langle\mathbf{M}^2\rangle}{3Vk_{\text{B}}T} \quad (5)$$

where \mathbf{M} is the total dipole moment of the sample, V is the volume of the sample, and the angular brackets indicate a time average. Several runs of 200 ps duration using the parameters in Table 2 were made to estimate $\langle\mathbf{M}^2\rangle$. The values of ϵ range from 7.3 to 8.6. This is less than the experimental value of 13.6 quoted in ref 7 or 14 reported in ref 20. It should be noted that I implemented model A and reproduced the pressure and energy reported for that model and state point. However, a smaller value for the dielectric constant of 11.7 was found rather than 12.6 reported for model A, probably because of the longer simulations used here.⁷

The computed configurational energy of the liquid is -29.9 kJ/mol. This should be compared with the experimentally determined heat of vaporization of 25.5 kJ/mol.²¹ The $p\Delta v$ term in the heat of vaporization is 2.5 kJ/mol, so the configurational

energy is too negative by 6.5 kJ/mol. This difference appears to be inherent in the model based on site–site 12–6 Lennard-Jones interactions.

A possible next step in testing the interaction model would be to determine the liquid–vapor coexistence line for the model using a Monte Carlo based method such as the Gibbs ensemble²² or the transition matrix Monte Carlo²³ method. This will require some code development since polarizability is inherently a many-body effect that will complicate the Monte Carlo schemes. It will be necessary to redetermine all of the induced moments for each Monte Carlo step, and how to do this efficiently is an open question.^{24,25}

Another check would be to determine if this model is consistent with the experimentally determined crystal structure²⁶ as that would reveal any glaring inconsistencies between the parameters in Table 2 and the actual intermolecular interactions.

References and Notes

- (1) Rebstat, S.; Mayer, D. Ethylene Oxide in *Ullmann's Encyclopedia of Industrial Chemistry*, VCH: Weinheim, 1987; Vol. A10; pp 117–135.
- (2) Dever, J. P.; George, K. F.; Hoffman, W. C.; Soo, H. Ethylene Oxide in *Kirk-Othmer Encyclopedia of Chemical Technology*, Wiley: New York, 1994; Vol. 9 4th ed. pp 915–959.
- (3) Johnson, R. D., III Computational Chemistry Comparison and Benchmark Data Base, <http://srdata.nist.gov/cccbdb>. The CCCBDB contains links to experimental and computational thermochemical data for a selected set of 631 gas-phase molecules and tools for comparing experimental and computational ideal-gas thermochemical properties.
- (4) Stryjek, J. B. *Pol. Acad. Sci. Chem. Sci* **1966**, *14*, 307.
- (5) Hurly, J. J. *Int. J. Thermophysics* **2002**, *23*, 667. $B(T)$ is tabulated at <http://properties.nist.gov/semiprop>.
- (6) Maass, O.; Boomer, E. H. *J. Am. Chem. Soc.* **1922**, *44*, 1709.
- (7) Wieloposki, P. A.; Smith, E. R. *Mol. Phys.* **1985**, *54*, 467.
- (8) Cunningham, G. L., Jr.; Boyd, A. W.; Myers, R.; Gwinn, W. D.; Le Van, W. I. *J. Chem. Phys.* **1951**, *19*, 676.
- (9) Yaws, C. L.; Rackley, M. P. *Chem. Eng.* **1976**, *83*, 129.
- (10) Gray, C. G.; Gubbins, K. E. *Theory of Molecular Fluids, Volume 1: Fundamentals*; Oxford University Press: Oxford, 1984; p 208.
- (11) Private communication from J. D. Olson, The Dow Chemical Company.
- (12) Martyna, G. J.; Klein, M. L.; Tuckerman, M. *J. Chem. Phys.* **1992**, *97*, 2635.
- (13) Martys, N. S.; Mountain, R. D. *Phys. Rev. E* **1999**, *59*, 3733.
- (14) Frenkel, D.; Smit, B. *Understanding Molecular Simulation, From Algorithms to Applications*, 2nd ed.; Academic Press: New York, 2002; pp 292–303.
- (15) Hamer, E.; Sutter, H. H. *Z. Naturforsch. A* **1976**, *31*, 265.
- (16) Bogaard, M. P.; Buckingham, A. D.; Pierens, R. K.; White, A. H. *J. Chem. Soc., Faraday Trans. 1* **1978**, *74*, 3008.
- (17) Perera, L.; Berkowitz, M. L. *J. Chem. Phys.* **1991**, *95*, 1954.
- (18) Mountain, R. D. *J. Chem. Phys.* **1995**, *103*, 3084.
- (19) Böttcher, C. F. J. *Theory of electric polarization*, 2nd ed.; Elsevier: Amsterdam, 1973; Vol. I, pp 117–121.
- (20) Davidson, D. W.; Wilson, G. J. *Can. J. Chem.* **1963**, *41*, 1424.
- (21) Giaque, W. F.; Gordon, J. *J. Am. Chem. Soc.* **1949**, *71*, 2176.
- (22) Panagiotopoulos, A. Z. *J. Phys.: Condens. Matter* **2000**, *12*, R25.
- (23) Errington, J. R. *J. Chem. Phys.* **2003**, *118*, 9915.
- (24) Chen, B.; Siepmann, J. I. *Theor. Chem. Acc.* **1999**, *103*, 87.
- (25) Předota, M.; Cummings, P. T.; Chialvo, A. A. *Mol. Phys.* **2002**, *100*, 2703.
- (26) Luger, P.; Zaki, C.; Buschmann, J.; Rudert, R. *Angew. Chem., Int. Ed. Engl.* **1986**, *25*, 276.